THE OPTIMIZATION OF FULL BAND-GAPS
IN MULTILAYER FILMS

VETURIA CHIROIU[1], LIGIA MUNTEANU[1], CRISTIAN RUGINA[1], DAN DUMITRIU[1],
PIER PAOLO DELSANTO[2]

Abstract. The multilayer films are consisted of alternating layers of material with
different mechanical properties, following a triadic Cantor sequence. The extremely
low thresholds for subharmonic generation of ultrasonic waves has a significant
importance in the generation of the full band-gaps due to the nonlinear coupling between
the extended-mode (phonon) and the localized-mode (fracton) vibration regimes. In
this paper, the optimization is performed with respect to most important features of sonic
composites, such as the localized modes around interfaces and the size of the full
band-gaps. The case of a relevant uncertainty of the design parameters which may change
over frequency is taken into consideration. Uncertain parameters are related to the
local band-gaps and boundary conditions where the displacement and the traction vectors
can be discontinuous. Maximizing the full band-gaps is taken as the objective function,
while the constant volume of the structure is taken as the constraint. The results show
an unexpected influence of discontinuities upon the generation of the full band-gaps.

Keywords: dynamic optimization, multilayer film, full band-gap.

1. INTRODUCTION

The focus of this paper is the development and the application of a dynamic
optimization problem for designing of sonic composites that exhibit the full band-
gaps where the sound is not allowed to propagate due to complete reflections. The
multi-objective optimization problem is selected as core of the framework [1–3].
The object of the optimization is the size of the full band-gaps that are obtained by
overlapping on certain interval of frequencies of the local band-gaps. The full band-
gaps are the well-known Bragg reflections which occur at different frequencies inverse
proportional to the central distance between two scaterers [4–6].

A sonic composite is a finite size periodic or non-periodic array of scatterers
embedded in a homogeneous material, which has the property of prohibiting the
propagation of certain waves [7]. The propagation of waves inside sonic composites

---

[1] Institute of Solid Mechanics of the Romanian Academy, Bucharest
[2] Politecnico di Torino, DISAT – Dipartimento Scienza Applicata e Tecnologia, Italy

consists in gaps in the energy band structure where waves are forbidden to propagate in certain directions. These gaps represented by the absence of real wave vector for some ranges of frequencies, can extend to the generation of full band-gaps where the waves are prohibited to travel in any polarization, any direction and from any source [8]. The evanescent field is distributed across the boundary of the waveguide into the surrounding composite by several times the lattice constant [9–13].

The sound attenuating frequency bands are not determined by the distribution of layers of scatterers, but by their intrinsic structure [7, 14–19].
In this paper, a multilayer sonic film consisting of alternating layers of material with different mechanical properties following a triadic Cantor sequence, is analyzed with respect to some design parameters which exhibit a relatively high degree of uncertainties. Uncertain parameters are related to the local band-gaps and boundary conditions where the displacement and the traction vectors can be discontinuous. The optimization target is mmaximizing of the full band-gaps, while structural integrity is taken as the constraint. The property of Cantor structures to generate the subharmonic waves is proving to be importance in the generation of the full band-gaps.

2. FORMULATION OF THE PROBLEM

The governing equations are given in [18].
The motion equations:

$$\rho^p \ddot{u}_i = t_{ij,j}, \quad \rho^e \ddot{u}_i = t_{ij,j}, \quad D_{i,i} = 0, \quad E_i + \varphi_{,i} = 0, \tag{1}$$

where indexes p, e describe the piezoelectric and epoxy resin, respectively, ρ is the density, u_i is the displacement vector, t_{ij} is the stress tensor, D_i is the electric induction vector, E_i is the electric field and φ is the electric potential.

The constitutive equations:

$$t_{ij} = \lambda^p \varepsilon_{kk} \delta_{ij} + 2\mu^p \varepsilon_{ij} + A^p \varepsilon_{il} \varepsilon_{jl} + 3B^p \varepsilon_{kk} \varepsilon_{ij} + C^p \varepsilon_{kk}^2 \delta_{ij} - e_k^p E_k \delta_{ij} - \\ - \overline{e}_k^p E_k \varepsilon_{ll} \delta_{ij} - \overline{\overline{e}}_k^p E_k \varepsilon_{ll} \delta_{ij} - \overline{e}_k^p E_k \varepsilon_{ij}, \tag{2}$$

$$t_{ij} = \lambda^e \varepsilon_{kk} \delta_{ij} + 2\mu^e \varepsilon_{ij} + A^e \varepsilon_{il} \varepsilon_{jl} + 3B^e \varepsilon_{kk} \varepsilon_{ij} + C^e \varepsilon_{kk}^2 \delta_{ij}, \tag{3}$$

$$D_i = \overline{\varepsilon}_i^p E_i - \frac{1}{2} \overline{\varepsilon}_i^p E^2 - e_i^p \varepsilon_{kk} - \frac{1}{2} \overline{e}_i^p \varepsilon_{kk}^2 - \frac{1}{2} \overline{\overline{e}}_i^p \varepsilon_{kk}^2, \tag{4}$$

where $\varepsilon_{ij} = \frac{1}{2}(u_{i,j} + u_{j,i})$ is the strain tensor, λ^p, μ^p are the Lame constants, A^p, B^p, C^p are the Landau constants, $\overline{\varepsilon}^p, \overline{\varepsilon}_i^p (\overline{\varepsilon}_3^p = \overline{\varepsilon}_2^p = \overline{\varepsilon}_1^p)$ are the linear and

nonlinear dielectric constants, $e_i^p (e_3^p = e_2^p = e_1^p)$, $\overline{e}_i^p (\overline{e}_3^p = \overline{e}_2^p = \overline{e}_1^p)$ and $\overline{\overline{e}}_i^p (\overline{\overline{e}}_3^p = \overline{\overline{e}}_2^p = \overline{\overline{e}}_1^p)$ are the linear and nonlinear coefficients of piezoelectricity and $E^2 = E_1^2 + E_2^2 + E_3^2$.

We suppose that all quantities are independent with respect to x_2, and $u_2 = 0$, $E_2 = 0$,

$$u_1 = u_1(x_1, x_3, t), \ u_3 = u_3(x_1, x_3, t), \ E_1 = -\varphi_{,1}, \ E_3 = -\varphi_{,3}, \ \varphi = \varphi(x_1, x_3, t). \quad (5)$$

The boundary conditions:

$$t_{ij}^p n_j = \overline{T}_{ij} n_j = \overline{T}_i, \ \overline{T}_{ij} = \frac{1}{4\pi}(\overline{E}_i \overline{E}_j - \frac{1}{2}\overline{E}^2 \delta_{ij}), \ D_i n_i = \overline{d}, \ \varphi = \overline{\varphi}, \ t_{ij}^e n_j = 0, \quad (6)$$

where $\overline{T}_i, \overline{d}, \overline{\varphi}$ are quantities prescribed on the boundary and $\overline{T}_{ij}$ is the Maxwell stress tensor. The electric field $\overline{E}_i = \overline{E}_i^0 \exp(i\omega t)$ is applied to the both surfaces of the plate to excite the Lamb waves, over a wide frequency range ($10\text{kHz} < \omega/2\pi < 5\text{MHz}$). At the interfaces between constituents, the displacement and the traction vectors can be discontinuous

$$[u_1] = [u_3] \neq 0, \ \ [t_{11}] = [t_{13}] \neq 0, \quad (7)$$

where the bracket indicates a jump across the interface and $k = 1, 3$. These discontinuities are portrayed by interval mathematical theory.

3. THE BAND STRUCTURE OPTIMIZATION

The Bloch's theorem states that the response of a sonic composite with periodical scatterers is characterized by the response of the unit cell generator (a unit scatterer) which is used to build the composite in the repetitive way in order to obtain periodicity. The wave propagation in the composite can be described by the wave propagation in the unit scatterer [20]. For a periodic 2D sonic structure consisted of an array of rectangular acoustic scatterers embedded in an epoxy matrix. This structure is built as a repetition of a unit rectangular scatterer of length a and b in the directions d_1 and d_2. Each point P in the structure has a corresponding point Q in the unit scatterer. The structure is generated by translating a number of n_1 scatterers along d_1 and a number of scatterers n_2 along d_2

$$r_P = r_Q + n_1 d_1 + n_2 d_2. \quad (8)$$

Block Theorem. *The response $u(r_P, \omega)$ of a 2D periodic structure is expressed in terms of the response of the unit scatterer and an exponential term which defines the amplitude and the phase change of the wave propagating from one scatterer to the next*

$$u(r_P, \omega) = u_0(r_Q, \omega) \exp k(n_1 d_1 + n_2 d_2) \,. \tag{9}$$

where $u_0(r_Q, \omega)$ is the reference response of the unit scatterer, ω is the angular frequency and k is the wave vector.

The propagation vector $\mu(\mu_1, \mu_2)$

$$\mu = kd \,, \tag{10}$$

defines the complex phase shifts in the directions d_1 and d_2.

With (10), Eq. (9) becomes

$$u(r_P, \omega) = u_0(r_Q, \omega) \exp \mu \nu \,, \tag{11}$$

where ν is a vector which indicated the number of scatterers translated in both directions.

The aim is to maximise the full band-gap interval of frequencies in which waves cannot propagate in the film. The length of the plate is l, the width of the plate is d, and the thickness of the plate is $2h$. The width of the smallest layer is $a = l/3^{n+1}$, where n is the order of the Cantor sequence.

The uncertain parameters are related to the discontinuous displacements and traction vectors at the interfaces between constituents, and may vary over frequency. These discontinuities are portrayed by interval mathematical theory. Then the optimum design is carried out under interval uncertainty for (7)

$$[\bar{u}_1] = [\bar{u}_3] = r(\omega), \quad [\bar{t}_{11}] = [\bar{t}_{13}] = s(\omega), \tag{12}$$

with $\bar{u}$ and $\bar{t}$ dimensionless displacement and stress, respectively, and $r(\omega), s(\omega)$ real functions depending on frequency $\omega \in [\omega_1, \omega_2]$.

The object of optimization is a function of eigenfrequencies and the constraint is that the volume is constant. The eigenfrequencies are found by solving the eigenfrequency problem

$$(S - \omega^2 M)D = 0 \,, \tag{13}$$

where S is the total stiffness matrix, ω^2 the squared eigenfrequency, M the total mass matrix and D the eigenvector.

The key of the band-gap generation is the lack of purely real wave vector for certain modes of waves at certain frequencies. The wave amplitude may decay exponentially sustaining an evanescent mode. Therefore, by aassuming free wave

propagation for which propagation vector is strictly imaginary, Eq. (13) is solved with respect to the angular frequency ω.

We know that the Bragg reflections occur at different frequencies inverse proportional to the constant *a*. If the local band-gaps are not wide enough, their frequency ranges do not overlap. The overlapping is due to reflections on the interfaces. Then, any wave is reflected completely from this structure in the frequency range where all the local band-gaps for the different periodical directions overlap. This is the mechanism of generation the full band-gap. The complete reflection on the boundaries is due to the full band-gap property itself, independent of the incident angle. This makes sharp bends of the wave-guide in the film. The evanescent waves distribute across the interfaces of the waveguide into the surrounding composite by several times the quantity *a*.

Let us to introduce a weighting index which can vary during the optimization procedure with respect to frequency

$$W_j = \exp\left| -K(\omega) \frac{\left(L_{i+j}^2 \cap L_i^2 \right)}{L_i^2} \right| , \quad i, j = 1, 2, ..., M \tag{14}$$

where L_i is the size of the *i*-th local band-gap, *M* is a number large enough to include all possible candidates band-gaps ready to be overlapped, *K* a given constant depending on the frequency. The weighting index characterises the size of the local band-gaps and the mechanism of the overlapping.

The resonant Lamb modes are excited by applying an external electric field $\bar{E}_1 = \bar{E}_3 = \bar{E}^0 \exp(i\omega_0 t)$ on both sides of the plate. The surface Lamb waves are superposition of longitudinal (symmetric waves) and shear modes (anti-symmetric waves or SV waves), which dominate the radial in-plane and vertical motion of particles in the film. The structure and size of the band-gap depend on $\bar{E}^0$. If $\bar{E}^0$ is increased above a threshold value $\bar{E}_{th}^0$, the $\omega/2$ subharmonic generation is observed. The result of superposition of normal and subharmonic modes is the generation of two kind of vibration regimes: a localised-mode (fracton) regime and an extended-vibration (phonon) regime [18, 19]. The fracton vibrations are mostly localised on a few elements, while the phonon vibrations essentially extend to the whole film. For the homogeneous plate the mismatch $\omega_n - \omega/2$ is due to the symmetry of fundamental modes with respect to *x*. Only symmetric odd *n* can induce a subharmonic, but never $\omega/2$ coincides with a plate vibration mode.

4. MAIN RESULTS

The calculus is carried out for $l = 68$ mm and $\bar{E}_{th}^0 = 5.27$ V. The material constants for piezoelectric ceramics and epoxy resin are shown in Table 1. Table 2

shows the computed frequencies and the errors obtained before optimization, in the absence of the discontinuities, for $n = 3$ [21,22]. The functions $r(\omega)$ and $s(\omega)$ are described in Fig. 1.

Table 1

The material constants for piezoelectric ceramics and epoxy resin

	piezoelectric ceramics	epoxy resin
λ [GPa]	71.6	42.31
μ [GPa]	35.8	3.76
A [GPa]	-2000	2.8
B [GPa]	-1134	9.7
C [GPa]	-900	-5.7
$\overline{\varepsilon}$ [nF/m]	4.065	-
$\overline{\varepsilon}_1$ [nF/m]	2.079	-
e_1 [nm/V]	-0.218	-
$\overline{e}_1 = \overline{\overline{e}}_1$ [nm/V]	-0.435	-
ρ [kg/m^3]	7650	1170

Table 2

Estimation results: computed eigenfrequencies $\omega_n / 2\pi$ for $n = 3$

100.2 ± 0.05	167 ± 0.01	217.1 ± 0.03	250.5 ± 0.1	334 ± 0.01	367.4 ± 0.01	417.5 ± 0.1	501 ± 0.02	584.5 ± 0.03
617.9 ± 0.01	668 ± 0.03	835 ± 0.06	935.2 ± 0.06	1085.5 ± 0.1	1169 ± 0.07	1269.2 ± 0.02	1503 ± 0.05	1670 ± 0.4
1770.2 ± 0.2	1987.3 ± 0.12	2120.9 ± 0.02	2250 ± 0.1	2471.6 ± 0.3	2655.3 ± 0.01	2672 ± 0.01	2972.6 ± 0.2	3340 ± 0.4

The optimisation algorithm is solved by a genetic algorithm. The first computed eigenfrequencies for $n = 3$ ($\omega_1 = 100$ Hz, $\omega_2 = 600$ Hz) and $n = 4$ ($\omega_1 = 130$ Hz, $\omega_2 = 600$ Hz) for maximum values of discontinuities, and minimum values of the discontinuities, respectively, are shown in Table 3. A significant reduction of frequencies, especially for maximum values of discontinuities is observed.
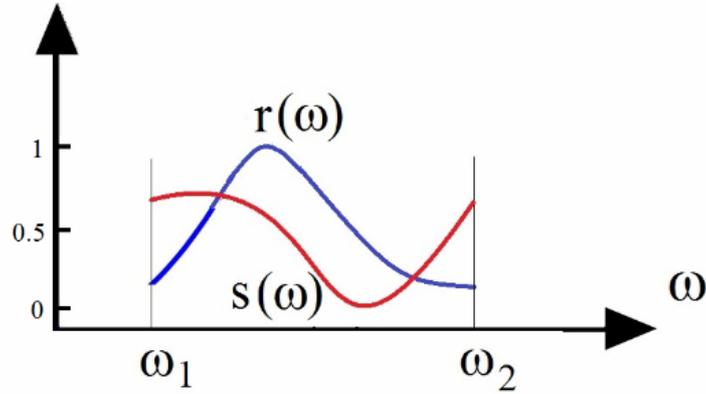
Fig.1 – Functions r(ω) and s(ω).

Table 3

Computed eigenfrequencies for $n = 3$ and $n = 4$,
in the presence of discontinuities

$\omega/2\pi$ [Hz] $n = 3$ maximum of discontinuities	$\omega/2\pi$ [Hz] $n = 3$ minimum of discontinuities	$\omega/2\pi$ [Hz] $n = 4$ maximum of discontinuities	$\omega/2\pi$ [Hz] $n = 4$ minimum of discontinuities
81.7 ± 0.03	89.2 ± 0.06	102.4 ± 0.01	112.1 ± 0.01
$98 \ \ \pm 0.01$	$107 \ \ \pm 0.01$	155.5 ± 0.01	161.1 ± 0.02
131.9 ± 0.05	155.4 ± 0.06	201.7 ± 0.02	211.5 ± 0.03
212.0 ± 0.1	232.9 ± 0.1	239.7 ± 0.2	244.1 ± 0.1
$253 \ \ \pm 0.1$	$274 \ \ \pm 0.1$	311.7 ± 0.1	300.4 ± 0.1
287.0 ± 0.02	307.4 ± 0.03	$389 \ \ \pm 0.02$	$377 \ \ \pm 0.03$
400.1 ± 0.1	440.8 ± 0.1	400.4 ± 0.01	423.8 ± 0.02
439.5 ± 0.03	486.1 ± 0.02	487.7 ± 0.03	504.0 ± 0.02
504.3 ± 0.02	554.5 ± 0.01	525.0 ± 0.1	580.5 ± 0.1

Figure 2 presents the variation of the index *W* with respect to the maximum size of the full band-gap for n = 3 and 4, respectively. The maximum size of the full band-gap is calculated as the difference max($\omega a / 2\pi c_0$) – min($\omega a / 2\pi c_0$), for a given $ka/2\pi$, with c_0 is the speed of sound in air, and $a = l/3^{n+1}$. We draw from this figure the conclusion that the size of the band-gap is favoured for *n* = 4, for which $2h = 0.25$ mm and $d = 25$ mm, $M = 120$. The value $K = 4.56$ was calculated by choosing for *W* the value corresponding to maximum full band-gap size ($W = 10.68$).

Figure 3 shows the full band-gap for $n = 3$ ($\omega = 81.7$ Hz, $W = 8.52$ and $K = 4.33$) and $n = 4$ ($\omega = 102.4$ Hz, $W = 10.68$ and $K = 4.56$), respectively.

Analysing the effect of the constant K on the results, the influence becomes important due to the contribution of the subharmonic waves in the generation of the full band-gaps. The spatial matching of coupled modes and the superposition of normal and subharmonic modes depend on K.
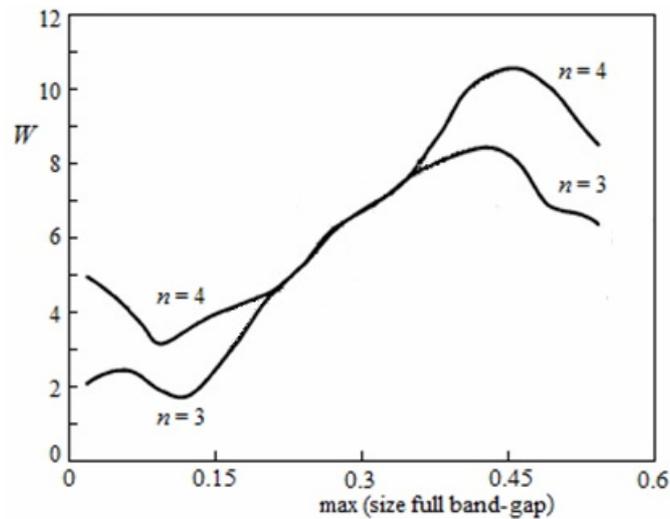

Fig. 2 — The index W with respect to the maximum size of the full band-gap for $n = 3$ and 4.
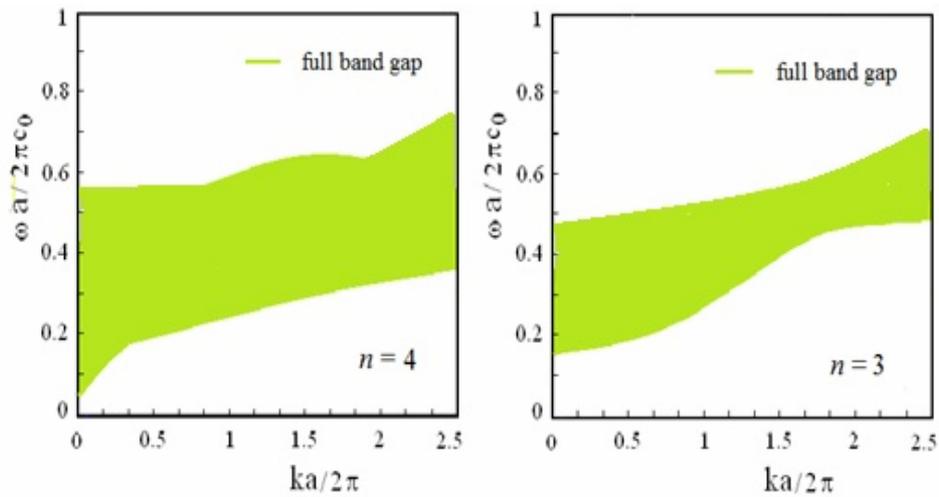
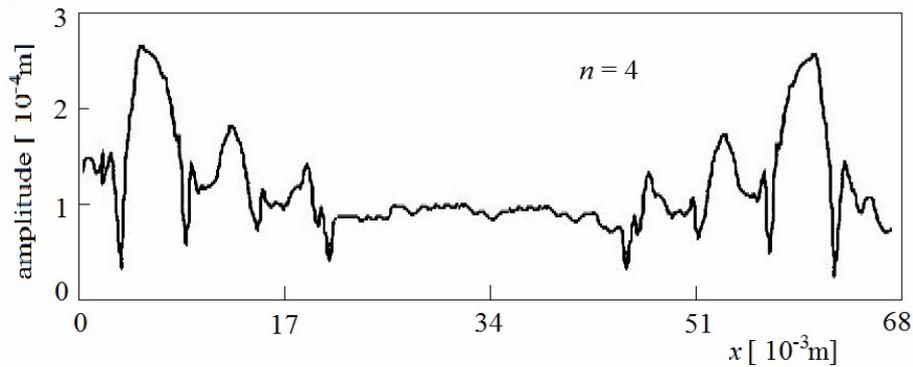Fig. 3 — The full band-gaps for $n = 3$ and $n = 4$.

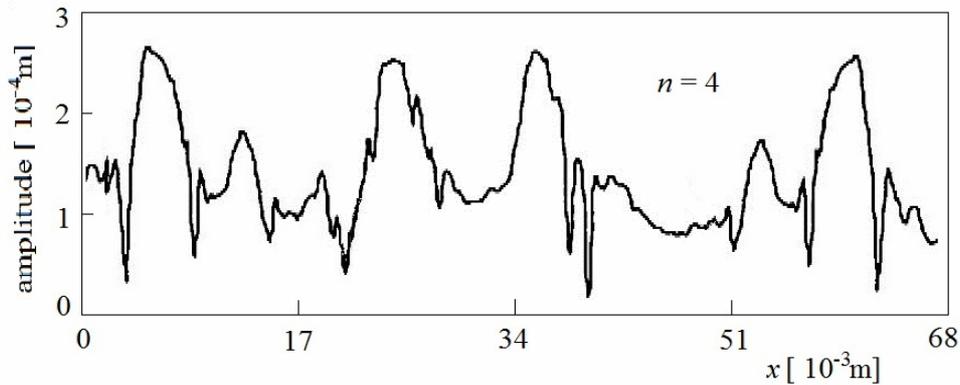Fig. 4 − The fracton regime for $n = 4$ for $K = 4.56$ and $\omega/2\pi = 102.4$ Hz.

Fig. 5 − The phonon regime
for $n = 4$ for $K = 4.56$ and $\omega/2\pi = 155.5$ Hz.

To understand this phenomenon, we display in Fig. 4 the fraction-vibration behaviour for $\omega/2\pi = 171.3$ Hz, and in Fig. 5 the extended-vibration behaviour, for $\omega/2\pi = 231.9$ Hz and $K = 4.56$. For $K = 4$, we see that the things are changing. Even if the fracton mode gives no differences, there are some changes in the phonon mode, in particular for the edge of the film. The phonon regime for $n = 4$ for $K = 4$ and $\omega/2\pi = 200.4$ Hz.

The variation of the maximum size of the full band-gap as function of minimum and maximum values of discontinuities, respectively, is presented in Fig. 6, for $n = 4$ and $\omega/2\pi \in [100\,\text{Hz}, 500\,\text{Hz}]$. We observe that presence of discontinuities improves the size of the full band-gaps. The optimal size for full band-gaps is obtained for maximum values of discontinuities rather than for small values of the discontinuities.
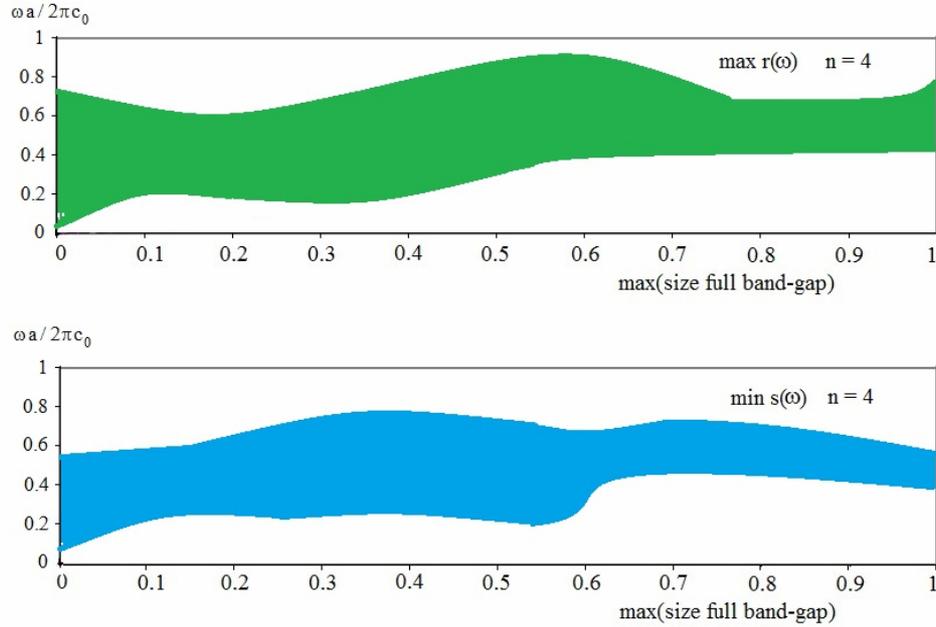
Fig. 6 – Variation of the size of the full band-gaps
with respect to minimum and maximum values of the discontinuities, respectively.

5. CONCLUSIONS

The paper presents the optimization of multilayer sonic films consisted of alternating layers of material with different mechanical properties following a triadic Cantor sequence. This structure has the ability to generate the subharmonic waves which have a significant importance in the generation of the full band-gaps where waves are not allowed to propagate. The rationale for the band-gap generation is the lack of purely real wave vector for certain modes of waves at certain frequencies and in consequence, the evanescent waves distributed across the boundary of the waveguide.

The objective of optimization is the maximization of the full band-gaps for uncertainty of the boundary conditions for which the displacements and the traction vectors can be discontinuous. The uncertain parameters are related to the discontinuous displacements and traction vectors at the interfaces between constituents, and may vary over frequency. Maximizing the full band-gaps is taken as the objective function, while the constant volume of the structure is taken as the constraint. The results show an unexpected influence of discontinuities upon the generation of the full band-gaps. An optimal size for full band-gaps is obtained for maximum values of discontinuities rather than for small values of the discontinuities.

The optimisation algorithm is solved by a genetic algorithm. The nonlinear coupling between the phonon and the fracton vibration regimes, accelerates the process of overlapping of the local full band-gaps, and the presence of discontinuities improve the size of the full band-gaps.

Received on May 22, 2016

REFERENCES

1. MIETTINEN, J., *Nonlinear Multiobjective Optimization*, Springer-Verlag, 1999.
2. HWANG, C-L., MASUD, A.S.M., *Multiple objective decision making, methods and applications*: *A state-of-the-art survey*, Springer-Verlag, 1979.
3. TRAPANI, G., KIPOUROS, T., SAVILL, A.M., *The design of multi-element airfoils through multi-objective optimization techniques*, CMES: Computer Modeling in Engineering & Sciences, **88**, *2*, pp. 107–140, 2012.
4. KAFESAKI, M., ECONOMOU, E.N., *Interpretation of the bandstructure results for elastic and acoustic waves by analogy with the LCAO approach,* Phys. Rev. B, **52**, *18*, pp. 13317–13331, 1995.
5. PSAROBAS, I.E., STEFANOU, N., MODINOS, A., *Scattering of elastic waves by periodic arrays of spherical bodies*, Phys. Rev. B, **62**, *1*, pp. 278–291, 2000.
6. MARTÍNEZ-SALA, R., SANCHO, J., SÁNCHEZ, J.V., GÓMEZ, V., LLINARES, J., MESEGUER, F., *Sound attenuation by sculpture*, Nature, **378**, p. 241, 1995.
7. HIRSEKORN, M., DELSANTO, P.P., BATRA, N.K., MATIC, P., *Modelling and simulation of acoustic wave propagation in locally resonant sonic materials*, Ultrasonics, **42**, *1*, pp. 231–235, 2004.
8. JOANNOPOULUS, J.D., JOHNSON, S.G., WINN, J.N., MEADE, R.D., *Photonic Crystals. Molding the Flow of Light*, Princeton University Press, 2008.
9. MIYASHITA, T., TANIGUCHI, R., SAKAMOTO, H., *Experimental full band-gap of a sonic-crystal slab structure of a 2D lattice of aluminum rods in air*, Proc. 5th World Congress on Ultrasonics TO-PM04.02, 2003.
10. MIYASHITA, T., *Full band gaps of sonic crystals made of acrylic cylinders in air-numerical and experimental investigations*, Jpn. J. Appl. Phys. **41**, *5S*, p. 3170.
11. GOFFAUX, C., SANCHEZ-DEHESA, J., *Two-dimensional phononic crystals studied using a variational method: application to lattices of locally resonant materials*, Phys. Rev. B, **67**, *14*, p. 144301, 2003.
12. GOFFAUX, C., MASERI, F.,VASSEUR, J.O., DJAFARI-ROUHANI, B., LAMBIN, P., *Measurements and calculations of the sound attenuation by a phononic band gap structure suitable for an insulating partition application*, Appl. Phys. Lett., **83**, *2*, pp. 281–283, 2003.
13. GUPTA, B.C., YE, Z., *Theoretical analysis of the focusing of acoustic waves by two-dimensional sonic crystals*, Phys. Rev. E., **67**, *3*, p. 036603, 2003.
14. LIU, Z., ZHANG, X., MAO, Y., ZHU, Y.Y., YANG, Z., CHAN, C.T., SHENG, P., *Locally resonant sonic materials*, Science, **289**, *5485*, pp. 1734–1736, 2000.
15. CHIROIU, V., BRIŞAN, C., POPESCU, M.A., GIRIP, I., MUNTEANU, L., *On the sonic*

composites without/with defects, Journal of Applied Physics, **114**, *16*, p. 164909-1-9, 2013.

16. MUNTEANU, L., CHIROIU, V., DONESCU, ST., BRIŞAN, C., *A new class of sonic composites*, Journal of Applied Physics, **115**, *10*, p. 104904, 2014.

17. MUNTEANU, L., CHIROIU, V., SERBAN, V., *From geometric transformations to auxetic materials*, CMC: Computers, Materials & Continua, **42**, *3*, pp. 175–203, 2014.

18. MUNTEANU, L., CHIROIU, V., SIRETEANU, T., DUMITRIU, D., *A multilayer sonic film*, Journal of Applied Physics, **118**, *16*, p.165302, 2015.

19. MUNTEANU, L., MOSNEGUŢU, V., CHIROIU, V., ILIE, R., *The cnoidal method with application to sonic composites*, Scientific Bulletin, University Politehnica of Bucharest, Series A, **77**, *3*, pp. 271–284, 2015.

20. CLAEYS, C.C., VIVOLO, M., SAS, P., DESMET, W., *Numerical and experimental study of local cell resonators to obtain low-frequency vibrational stopbands in periodic lightweight structures* (Chapter 4), in: *Topics in Modal Analysis II*, Vol.6, Conference Proceedings of the Society for Experimental Mechanics Series, The 30th IMAC, A Conference on Structural Dynamics, Jacksonville, Florida (Springer), 2012.

21. CHIROIU, C., DELSANTO, P.P., SCALERANDI, M., CHIROIU, V., SIRETEANU, T., S*ubharmonic generation in piezoelectrics with Cantor-like structure,* Journal of Physics D: Applied Physics, Institute of Physics Publishing, **34**, *3*, pp. 1579–1586, 2001.

22. SCALERANDI, M., DELSANTO, P.P., CHIROIU, C., CHIROIU, V., *Numerical simulation of pulse propagation in nonlinear 1-D media*, Journal of the Acoustical Society of America, **106**, *5*, pp. 2424–2430, 1999.